Eng. Sci., 2022, **20**, 352–363

Engineered Science

DOI: https://dx.doi.org/10.30919/es8e765

Two-way Fluid-Structure Interaction Analysis of Single Pad Externally Adjustable Fluid Film Bearing

Harishkumar Kamat,[1,#] Chandrakant R. Kini[2,#] and Satish B. Shenoy[2,#,*]

Abstract

One of the present industrial requirements is the development of high-speed, high-load-carrying capacity machines. The problem of instability in high-speed conventional fluid film bearings can be prevented with the use of externally adjustable fluid film bearings. In the present study, the elastohydrodynamic behavior of a single pad externally adjustable fluid film bearing is reported for radial and tilt adjustment of the pad in the upward direction. Using the computational fluid dynamics (CFD) technique, a numerical study has been performed to measure fluid pressure generation for various eccentricity ratios. Later bearing deformation and stresses developed in the bearing are predicted using ANSYS commercial software. The current numerical method, which can be used to solve complex bearing models, has been evaluated against previously published literature, and the findings are in good agreement. The results of the CFD study indicate that bearing performance is superior when the pads are adjusted in the upward direction at a larger eccentricity ratio. Under the same geometric modification, design parameters such as fluid pressure, pad deformation, and stresses are evaluated and compared using the one-way and two-way fluid-structure interaction (FSI) technique. These two-way FSI results help in the bearing design stage.

Keywords: Externally adjustable fluid film bearing; CFD; One-way FSI; Two-way FSI; Single pad.
Received: 16 June 2022; Revised: 13 August 2022; Accepted: 18 August 2022.
Article type: Research article

1. Introduction

Bearings are critical components in modern high-speed turbomachinery as they need to support high loads with better performance characteristics at a lower power dissipation. The bearing clearance area must be lowered to ensure optimal performance with minimal power dissipation. On the other hand, this reduction in bearing clearance will increase heat generation, oil whirl, and oil whip, decreasing load-carrying capacity. Although all existing circular bearings with fixed sleeves improve bearing performance slightly, researchers have proved that in fluid film bearings, temperature rise, instability at high speed, and oil whirl /whip are some of the significant disadvantages of using them. Hence, to eliminate such difficulties, development in noncircular bearing has started, and attention is being focused on alternative noncircular bearings. One such noncircular bearing is an adjustable pad bearing also known as externally adjustable pad fluid film (EAFF) bearing, where the hydrodynamic effect can be altered continuously in an organized manner during operation.

In EAFF bearings, hydrodynamic conditions can be altered continuously in a controlled manner during operation.[1] The primary principle feature of these bearings is to modify the radial clearance and film thickness along the circumferential direction. The radial clearance and film thickness gradient can be altered by providing controlled tilt and radial adjustments to the bearing pads. Pads can be adjusted externally via sensors, spacers, or oil injection.[1–3] Controlled position inputs are provided in a radial direction and some tilting movements along the leading edge. Compared with partial arc bearings, these adjustable pad bearings have superior performance features such as higher speeds, lower power absorption, and improved stability characteristics. When the pad adjustment is set to zero, the partial arc bearing performance is comparable

[1] *Department of Mechanical and Industrial Engineering, Manipal Institute of Technology, Manipal Academy of Higher Education, Manipal, Karnataka, 576104, India.*
[2] *Department of Aeronautical and Automobile Engineering, Manipal Institute of Technology, Manipal Academy of Higher Education, Manipal, Karnataka, 576104, India.*
[#]All these authors contributed equally to this work.
**E-mail:* satish.shenoy@manipal.edu (S. B. Shenoy)

to an externally adjustable fluid film bearing.[1] Externally adjustable single pad fluid film bearings are used in high-speed, high-load applications such as turbines and marine propulsion systems to achieve greater stiffness with less power dissipation.

In bearing, hydrodynamic fluid pressure can be generated when the two surfaces move relative to one another forming a convergent wedge. The magnitude of the hydrodynamic pressure depends on the geometrical details of the wedge and fluid viscosity. High fluid film pressure bearings have a high load-carrying capability, but they also risk distorting the surfaces and changing the film domain. Consideration of elastic distortion in the study of hydrodynamic lubrication is called elastohydrodynamic lubrication (EHL). Yiping *et al.*,[4] Shenoy *et al.*,[5] Liu *et al.*,[6] Gao *et al.*,[7] Chen *et al.*,[8] Lin *et al.*,[9] and Li *et al.*[10] highlighted the importance of EHL in journal bearing. Many researchers have conducted numerical and experimental studies on circular journal bearings and investigated the performance parameters. Gertzos *et al.*[11] Bompos, Nikolakopoulos, and others[12,13] performed the computational fluid dynamics (CFD) analysis of journal bearing using smart lubricants like Bingham, magnetorheological and electrorheological fluids, respectively. Yiping *et al.*[4] developed a fluid-structure interaction (FSI) model to capture the behavior of lubricant and stress distribution in the bearing. Shenoy *et al.*[5] investigated the effect of eccentricity ratio on bearing performance and studied the structural deformation in journal bearing using the FSI technique. A similar FSI technique is used by Liu *et al.*[6] to highlight the influence of using different bearing materials on the load carrying capacity of journal bearing and concluded that bearing with low Young's modulus deforms more than other bearing materials. Gao *et al.*[7] developed a design reference chart to select water lubricated journal bearing using CFD and FSI techniques. Using a similar technique, researchers like Chen *et al.*[8] and Lin *et al.*[9] studied the influence of the number of oil grooves and their location on the bearing deformation. They have concluded that the number of grooves and locations are key in altering elastohydrodynamic lubrication (EHL) characteristics of journal bearing. Li *et al.*[10] captured the transient flow behavior of lubricant inside the double groove journal bearing system using the CFD-FSI method. FSI method is also incorporated to study the tilting pad bearing by Geller *et al.*[14] considering the multiphase flow.

In 1998, Martin and Parkins patented the adjustable pad bearing design to control the hydrodynamic operation. Later, Martin[15] derived Reynolds equations for this pad bearing considering the nonuniform variation in the film thickness direction. In 2008, Shenoy and Pai used the proposed novel bearing principle to predict the static bearing performance parameters in both laminar and turbulence conditions[16] and the presence of rotor misalignment.[17] The same authors extended the theoretical approach to predict dynamic characteristics using the linearized perturbation method.[18] Pai and Parkins[19] conducted an experimental investigation into the performance parameters of a four pad EAFF bearing under various tilt and radial adjustments of the pad and concluded that these bearings are more stable than conventional bearings. Later, Hariharan and Pai performed detailed theoretical research on four pad EAFF bearings and investigated the rotor misalignment and the influence of offset load on bearing performance parameters.[20]

Similarly, Hariharan and Pai studied the steady-state performance of these pad bearings.[21] Bhat *et al.*[22] conducted an FSI analysis using an interchangeable spacer for 60° partial arc bearing with radial pad adjustment. The analysis is carried out for various bearing length (L)-to-diameter (D) ratios and eccentricity ratios by equating all the negative pressures to zero (*i.e.*, zero cavitation condition) under isothermal conditions. It was concluded that hydrodynamic pressure and stresses developed in the bearing are much higher when the partial arc bearing is given with radial adjustment in the upward direction. This is primarily due to decreased clearance gap between the shaft and bearing. All studies on externally adjustable four-pad bearings have found that the bearing performance is superior when the pads are adjusted in the upward (negative) direction. The significance of various cavitation models and the development of cavitation in fluid film bearing were discussed by Braun and Hannon.[23] The JFO model and Elrod cavitation model were found to be the most suitable models compared to the Sommerfeld model, Gumbel model, and Swift-Stieber model because they take mass continuity into account. Vijayaraghavan and Keith[24] modified Elrod's cavitation model to increase computational efficiency. Additionally, the Zwart-Gerber-Belamri cavitation model is largely used in numerical investigations, which accurately forecasts performance, displays good convergence behavior, and captures more realistic cavitation behavior compared to other numerical models.

FSI plays an important role in engineering and the medical industry, yet a challenging area of research. In recent decades, several computational techniques have been developed to address the challenges involved in FSI analysis. With the current technological developments in computers, complicated engineering problems can be solved. Due to the significant cost investment and limited scope for experiments related to FSI, many researchers are using numerical tools for

their analysis. It is impossible to get analytical solutions for complicated flows and geometry. Various researchers have used analytical and numerical methods such as the finite element method (FEM),[25–27] finite difference method (FDM),[28–30] and finite volume method (FVM)[31–33] to capture the flow characteristics in a journal bearing. The computational domain is discretized in these numerical methods into small segments, so-called control volumes. Later, the governing equations are discretized for each control volume and solved iteratively. Liu *et al*[6] highlighted the influence of bearing material by performing an FSI analysis. They concluded that bearing with lower Young's modulus (like nylon) deforms more than other bearing materials. Kamat *et al.*[34] performed the one-way FSI study on single pad EAFF bearing and concluded that pad deformation is quite high at a large eccentricity ratio under steady-state conditions. However, Kamat *et al.* did not consider the effect of pad deformation on the fluid properties. Incorporating two-way FSI on a single pad EAFF bearing for various tilt and radial pad adjustments is the main limitation of earlier research. In the present study, to avoid computing complexity and cost of performing a two-way FSI analysis, cavitation is allowed to occur by setting all the negative pressure generated in the fluid region equated to zero, as mentioned by researchers like Shenoy and Pai[16,17] Hariharan and Pai.[18,21]

The effectiveness of bearing lubrication is significantly influenced by elastohydrodynamic analysis; hence the FSI approach is used to investigate the elastohydrodynamic behavior. In the present study, using commercially available ANSYS software, CFD and fluid-structure interaction (FSI) analysis of externally adjustable single pad bearing is carried out under steady-state conditions operating in constant unidirectional loading. Initially, one-way FSI analyses are performed for a 60° single pad EAFF bearing with a length-to-diameter ratio of one under laminar conditions for various eccentricity ratios and pad adjustments, and the results are validated with Shenoy and Pai.[35] Following that, two-way FSI analysis is performed on the same bearing, with results presented in contour plots and graphs.

2. Fluid-Structure Interaction (FSI)

The behavior of the fluid will change when it comes in contact with the deformable bearing structure and it is denoted as the elastohydrodynamic lubrication (EHL) effect. Thus, studying the interactive effect between the fluid and structure is crucial as it will decide the bearing performance. In the current study, FSI analysis is performed using ANSYS workbench R19 by coupling the modules of structural mechanics and fluid dynamics modules. There are mainly two possibilities for fluid -structure analysis: one-way FSI and two-way FSI.

For one-way FSI, fluid loads such as fluid pressure from ANSYS Fluent, CFX, or Icepak are imported to the mechanical system without any intermediate software or scripts. The meshed structural part is solved for the structural analysis by importing fluid pressure values. However, for one-way FSI, remodeling of fluid domain based on structural deformation is unaccounted. In two-way FSI, data transfer occurs every time step/iteration between CFD and mechanical system, and flow is remodeled based on the structural deformation.

2.1 Geometry

The dimensional parameters of 60° single pad EAFF bearing and fluid properties utilized in the current study are provided in Table 1. Three cases of pad viz positive (Case A), zero (case B), and negative (case C) radial and tilt adjustments are considered to find out their impact on the bearing performance and structural deformation. The model shown in Fig. 1 is a

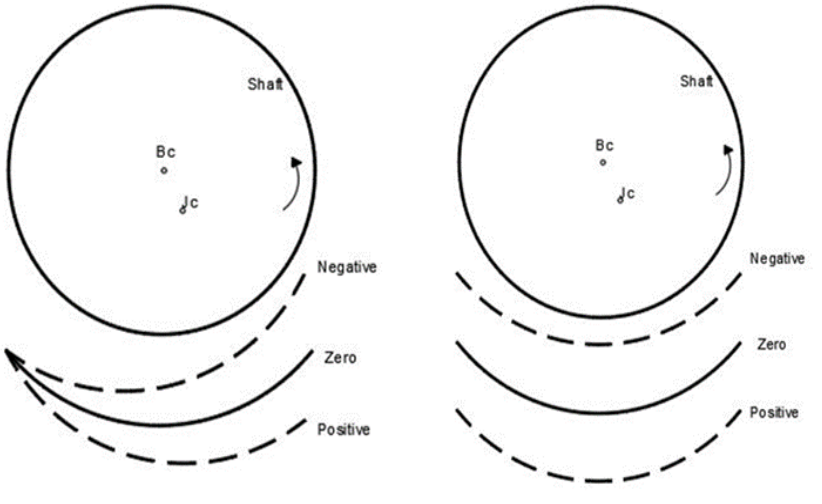

Fig. 1 Schematic diagram of externally adjustable single pad bearing (images are not as per the scale).

Table 1. Specification used for the present analysis.[36]

Parameters	Details		
Journal Radius (R)	0.0238 m		
Radial Clearance (C)	48 μm		
Pad thickness	10% of journal radius		
Radial Adjustment	Zero and ±25% of Radial clearance		
Tilt Adjustment	Zero and ± 0.0061°		
Pad Material Properties[37]	Bronze material Young's Modulus = 103.421359 GPa Poisson's ratio = 0.34		
Lubricant Viscosity (η)	$1.25e^{-2}$ Ns/m^2		
Lubricant density	840 kg/m^3		
Length to Diameter ratio (L/D)	1.0		
Eccentricity ratio (ε)	0.2, 0.4 and 0.6		
Operating Speed	124.92 rpm (Re 1)		
Pad configuration		Pad Adjustment	
		Tilt	Radial
	Case A	Positive	Positive
	Case B	Zero	Zero
	Case C	Negative	Negative

schematic representation of a 60° single pad EAFF bearing with the center of the bearing represented by 'B_c' and journal (or shaft) by 'J_c'. 'Φ' is the attitude angle, and radial distance between shaft center and journal center is denoted by 'e'. The constant external load (W) acts vertically downward on the journal running at a constant angular speed ('ω'). A small tilt adjustment (± 25% of radial clearance) at one corner of the pad can be given in a controlled manner. Similarly, the pad is adjusted in the radial direction by ±0.0061° to modify the bearing clearance.

2.2 Grid generation and boundary conditions

In the present study, mesh sensitivity is carried out for fluid film pressure and pad deformation at various element sizes using ANSYS FLUENT are presented in Figs. (2&3). Simulations are performed for element sizes varied from 0.5 mm to 0.1 mm for Case C pad adjustment. Figs. 2(a&b) depict the meshed model used in the present CFD and FEM solver, respectively. For the fluid domain, the plane was constructed at the mid-section of the fluid, and the fluid pressure values were obtained, whereas, for the solid domain, maximum bearing deformations were obtained at the pad's free end. The results demonstrate that the difference for the last two meh elements (0.1 mm and 0.08 mm) is less than 0.03 % in fluid pressure and deformation magnitudes as depicted in Figs. 3(a&b). Considering the computational time and efficiency of the results, an element size of 0.1 mm is selected for both fluid and solid domains with hexahedral mesh, as shown in Fig. 2.

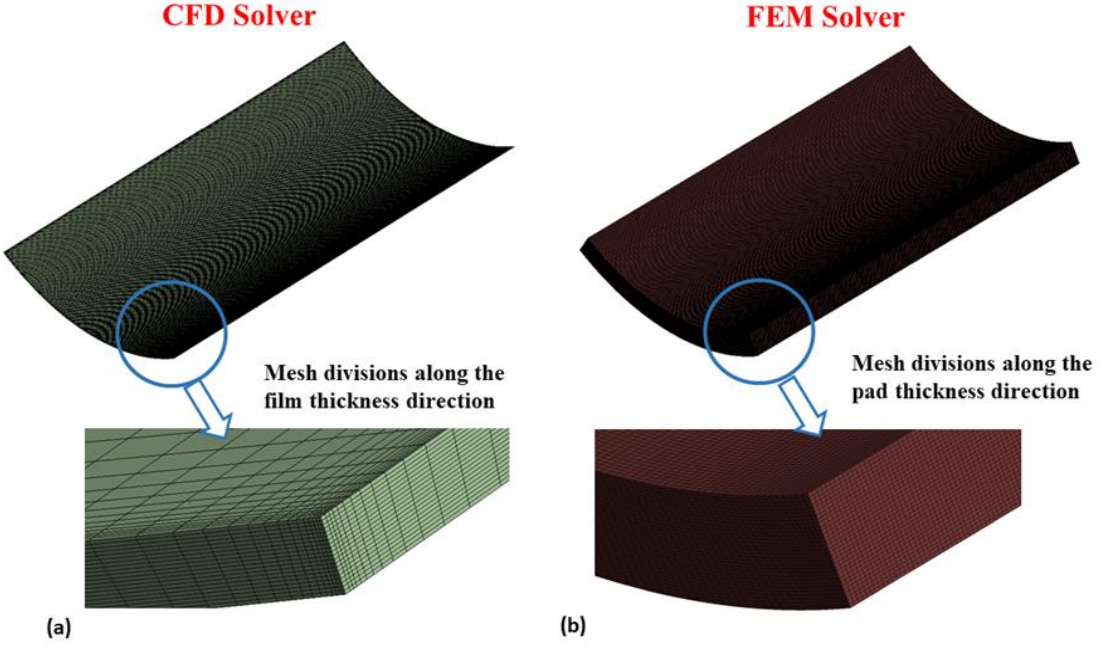

Fig. 2 Meshed model (a) fluid domain and (b) solid domain.

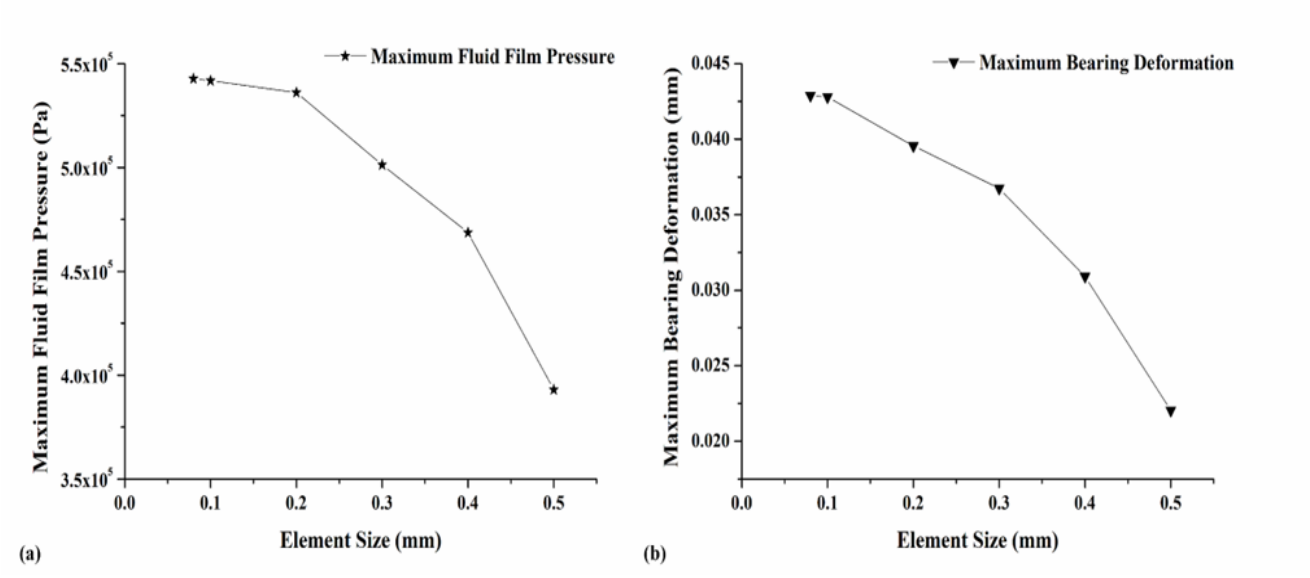

Fig. 3 Grid independence study (a) fluid domain and (b) solid domain.

Also, as the film thickness region is relatively small and significantly influences the bearing properties, Mesh refinement has been considered in that region (20 divisions).

During CFD analysis, the rotor or shaft is considered as moving wall boundary condition. The rotational axis origin of the shaft is set based on eccentricity and attitude angle values. One side of the film thickness region is set as a pressure inlet, and the remaining fluid faces are set as pressure outlet with zero-gauge pressure ($\overline{P_a}$) as shown in Fig. 4(a). Cavitation is allowed to occur by setting all the negative pressure generated in the fluid region is equated to zero by writing CFD code.

Figure. 4(b) represents the boundary conditions used for the solid domain. The leading edge of the pad bearing (*i.e.* θ = 0°) is given with fixed supports, the trailing edge of the pad (*i.e.* θ = 60°) is allowed to move freely and the pad behaves like a cantilever beam. Fluid pressure generated in the clearance region can act on the pad by coupling the respective fluid and solid region. The interface is created for the liquid and solid domains so that the transfer of energy occurs across the domain.

2.3 Governing equations

ANSYS Fluent, CFX, or any CFD software tool uses FVM to solve the governing equations for numerical solutions. Development in computer technologies helped researchers work on journal bearing using CFD and FSI techniques. The

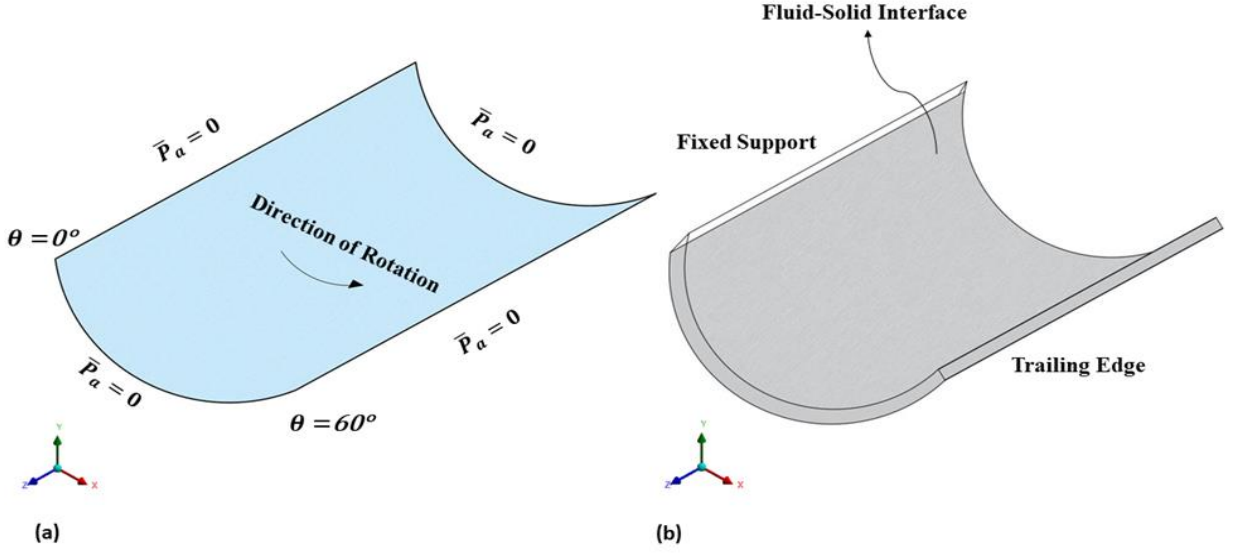

Fig. 4 Boundary condition used for (a) fluid model and (b) structural model.

authors used commercially available CFD software, ANSYS Fluent 19 R2.0 to solve full Navier-Stokes or momentum equation. ANSYS Fluent uses both equations of mass and momentum for computational fluid dynamics[38] to compute the velocity and pressure fields simultaneously. Equations (1) and (2) are given in the same order:

$$\nabla \times (\rho \vec{v}) = 0 \quad (1)$$

$$\nabla \times (\rho \overrightarrow{vv}) = -\nabla p + \nabla \times (\bar{\bar{\tau}}) + \rho \vec{g} \quad (2)$$

where p is the static pressure, $\bar{\bar{\tau}}$ is the stress tensor (described below), and $\rho \vec{g}$ is the gravitational body force, respectively. The stress tensor $\bar{\bar{\tau}}$ is given by Equation (3):

$$\bar{\bar{\tau}} = \mu \left[(\nabla \vec{v} + \nabla \vec{v}^T) - \frac{2}{3} \nabla \vec{v} I \right] \quad (3)$$

Where μ is the molecular viscosity, I is the unit tensor, and the second term on the right-hand side is the effect of volume dilation. For incompressible flow, $\nabla \vec{v} I$ becomes zero.

In two-way FSI, two solvers are utilized in which one solves the governing equations related to fluid, and another solver is used for the equation associated with the structure displacement. In this, these equations are solved sequentially. FSI analysis is achieved by using governing Equations (4) and (5)[39]: where 'K' is stiffness with suffix 's' and 'f' defining solid and fluid, respectively.

$$[M_S]\{\ddot{U}\} + [K_S]\{U\} = [F_S] + [R]\{P\} \quad (4)$$

$$\begin{bmatrix} M_S & 0 \\ \rho R^T & M_f \end{bmatrix} \begin{Bmatrix} \ddot{U} \\ \ddot{P} \end{Bmatrix} + \begin{bmatrix} K_S & -R \\ 0 & K_f \end{bmatrix} \begin{Bmatrix} U \\ P \end{Bmatrix} = \begin{Bmatrix} F_S \\ F_f \end{Bmatrix} \quad (5)$$

where $[M_S]$ and $[M_f]$ are the mass matrix for solid and fluid, respectively; $[F_S]$ and $[F_f]$ are the force matrix for solid and fluid respectively, and [R] is a coupling matrix.

2.4 Solution method

2.4.1 CFD

This section discusses the CFD approach employed in the current investigation with the help of ANSYS Fluent software. CFD techniques are used to measure the hydrodynamic fluid pressure generated in EAFF bearing and predict the lubricant behavior under steady-state conditions. The generated hydrodynamic fluid pressure is exerted onto the bearing pad surface, leading to deformation in the structure. This deformation results in the modification of the fluid flow regime. Hence, the dynamic remodeling technique of the flow is used to capture these physics. The smoothing and remeshing methods are used with a remeshing interval of 5. In the smoothing algorithm, the position of mesh nodes is altered, keeping the number of cells constant and limiting the decrease of mesh quality. FSI solution criteria such as convergence value, output frequency, and relaxation values are set up, and results are later checked and reviewed.

The conservation of momentum or Navier stokes equations are used and resolved by Fluent under a double-precision scheme. The first-order upwind scheme is used initially, and then later, for better accuracy higher-order upwind scheme is utilized. In addition, for pressure-based solvers, pressure values have been interpolated on the faces of the domain by a scheme called PRESTO. This scheme is adopted mainly to capture swirling flow or any steep pressure gradient in the flow domain. When the residuals in the calculation domain are less than 10^{-5}, the convergence of the solution is taken into account, with default under-relaxation parameters for all variables set as per ANSYS Fluent. General categories of numerical uncertainties are boundary conditions, complicated geometries, convergence criteria, and grids in the computing domain.[40] To strengthen the validity of the solution and lower uncertainty, the relevant numerical uncertainties for the current investigation such as validation of the CFD tool, and a grid sensitivity study was completed.

Simulation is carried out assuming the flow is steady, iso-viscous, isothermal, and has no-slip boundary condition. The bearing is also assumed to be perfectly aligned with VG-32 as a lubricant. Initially, CFD analysis is carried out by suppressing the solid domain, and moving wall boundary condition is used for the fluid domain in ANSYS fluent.

2.4.2 Methodology of FSI simulation

Figure 5 shows the flowchart of two-way FSI adopted in the present study using ANSYS workbench software. In the ANSYS workbench setting, the structural solver, which works based on the finite element method, and the computational fluid dynamic which utilizes the finite volume method are connected by a module called 'system coupling'. In this coupling, data transfer takes place in a controlled iterative manner between both fluid and solvers. At each iteration of the two-way FSI analysis, fluid and structure-related data between both solvers are exchanged.

During coupling iteration, initially in CFD, fluid forces are obtained by solving governing equations under the given boundary conditions and later these results are transferred to the structural solver. The structural solver calculates the stresses and deformation of a bearing using the information received from the fluid solver. These displacement results of the bearing are sent back to CFD solver to update the shape of the fluid domain, and flow equations are solved again. Hence, at each coupling iteration, the fluid computation domain is modified. To capture this modification in the fluid domain, the dynamic meshing technique is adopted, as explained earlier. The coupling iterations continue till the convergence is reached. Details of the data exchange between the fluid and the solid domain are shown in Fig. 5.

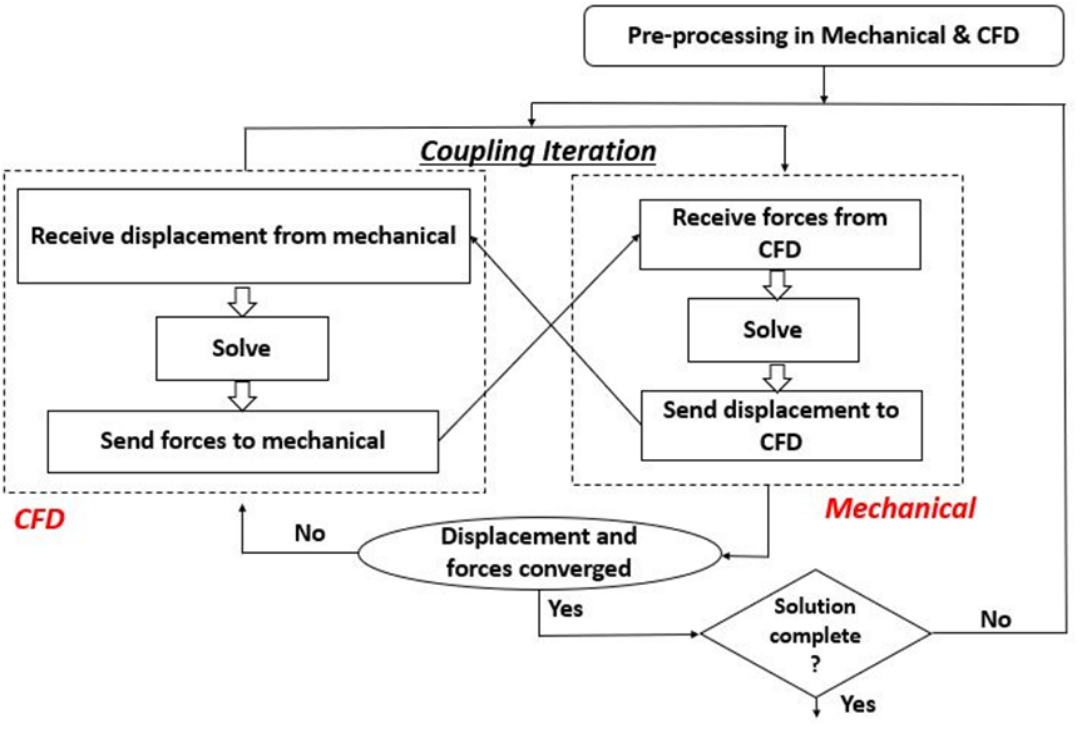

Fig. 5 Flow chart of two-way FSI solution technique.

3. Results and discussion

3.1 Validation of the CFD model

The performance of conventional partial arc bearing is identical to externally adjustable fluid film bearing when both radial and tilt adjustments are set to zero. To validate the simulation method, results obtained using the current CFD model are compared with the illustrations in Shenoy and Pai[35] for 60° single pad EAFF bearing with L/D = 1.0 with Reynolds number, Re = 1 for various eccentricity ratios with zero tilt and radial adjustment. They performed the analytical study on 60° single pad EAFF bearing at various tilt and radial adjustments and found that the influence of negative tilt and radial adjustment (Case C) on the bearing performance parameter is much greater than that of the other two cases. Fig. 6 compares the non-dimensional load carrying capacity as one of the bearing performance parameters with various eccentricity ratios. The present CFD results obtained for non-dimensional load carrying capacity are in good agreement with a deviation less than 2%.

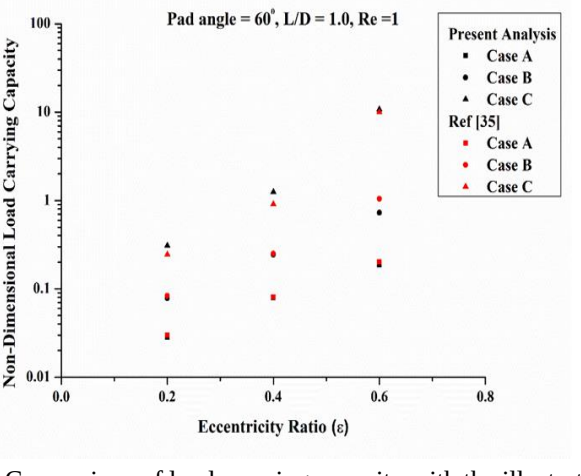

Fig. 6 Comparison of load carrying capacity with the illustrations in Shenoy *et al.*[35].

3.2 Two-way FSI Analysis

As in single pad EAFF bearing, performance parameters for case C (negative radial and negative tilt) are superior to the other two pad adjustments.[36] The two-way FSI analysis is performed for case C at various eccentricity ratios under steady-state conditions. The bearing deformation and stresses developed in the bearing due to fluid film pressure are evaluated via ANSYS R-19. Firstly, the fluid pressure values obtained in both one-way and two-way FSI results are compared, as shown in Figs. 7(a-e). It is evident from these figures that, for all eccentricity ratios, fluid pressure generated in two-way FSI is lower than that of one-way FSI. Further, it is observed that the fluid film pressure values are maximum at the midplane of the fluid region, these pressure values are extracted, and results are compared for both one-way and two-way FSI analysis as shown in Fig. S1. Secondly, bearing deformation in bearing are evaluated and color contour plots of the same are presented in Fig. 8.

On successful completion of flow analysis, fluid-structure interaction analysis is performed on externally adjustable single pad bearing for all three adjustment cases with various eccentricity ratios. Transfer of fluid pressure values onto the

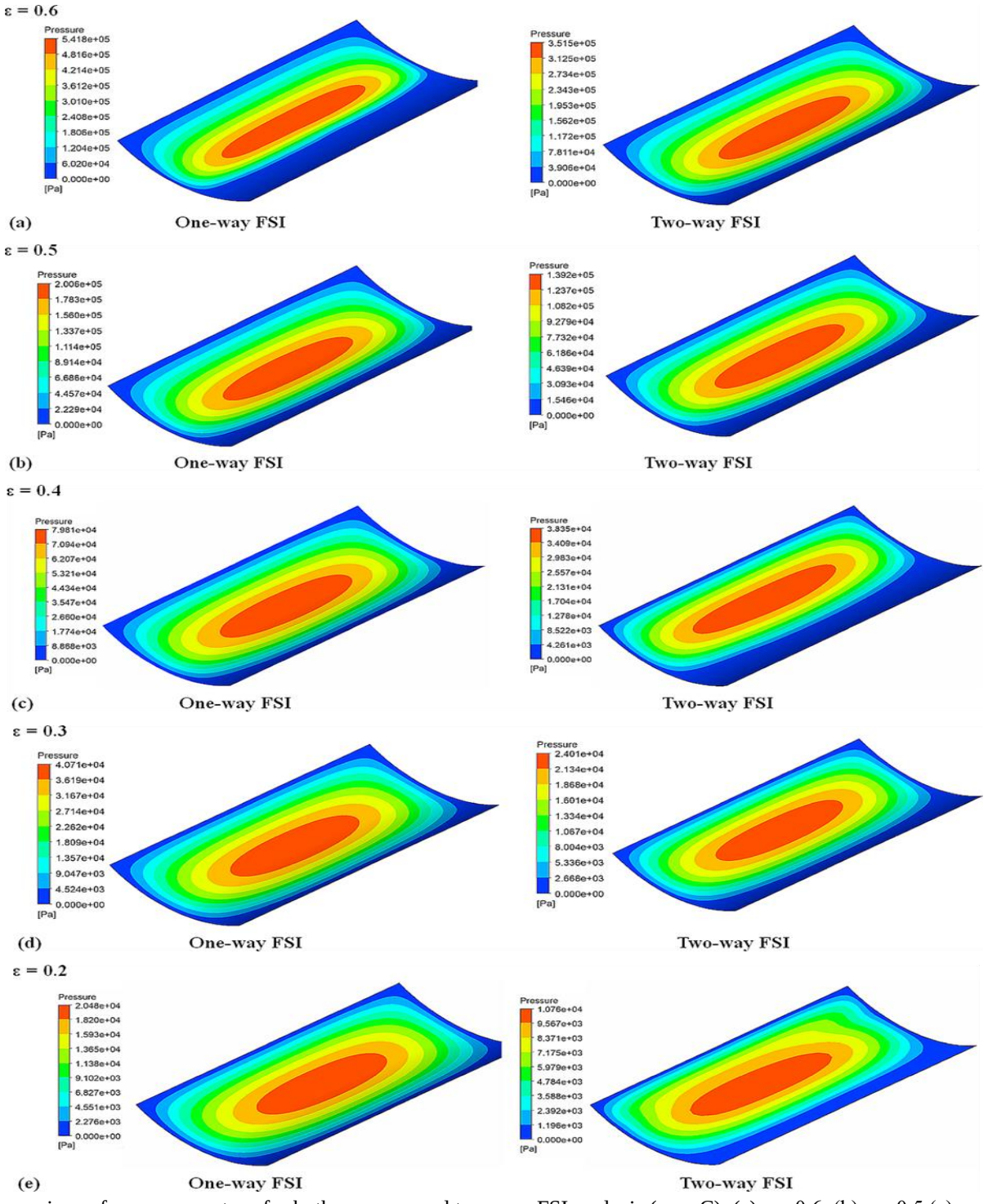

Fig. 7 Comparison of pressure contour for both one-way and two-way FSI analysis (case C): (a) ε = 0.6, (b) ε = 0.5 (c) ε = 0.4, (d) ε = 0.3 and (e) ε = 0.2.

respective region of pad bearing is performed after the strong coupling between CFD and structural mechanics. This fluid pressure acts like an external force acting on the pad bearing, leading to deformation in the structure. Results in terms of deformation, and stresses are extracted, and the critical region of the pad is determined.

A comparison of pressure distribution for one-way and two-way FSI for case C at ε = 0.6 are presented in Fig. 7(a). Similarly, Figs. 7(b-e) show the pressure contour plots of the FSI analysis for ε = 0.5 to 0.2. In comparison to the other eccentricity ratios, the magnitude of fluid pressure at ε = 0.6 is significantly higher. The primary cause for this is the reduction in clearance space between the bearing and shaft at higher eccentricity ratios.

From Fig. 7, the maximum fluid pressure in two-way FSI for = 0.6 is 3.515e5 Pa, a reduction of 54.13 percent is

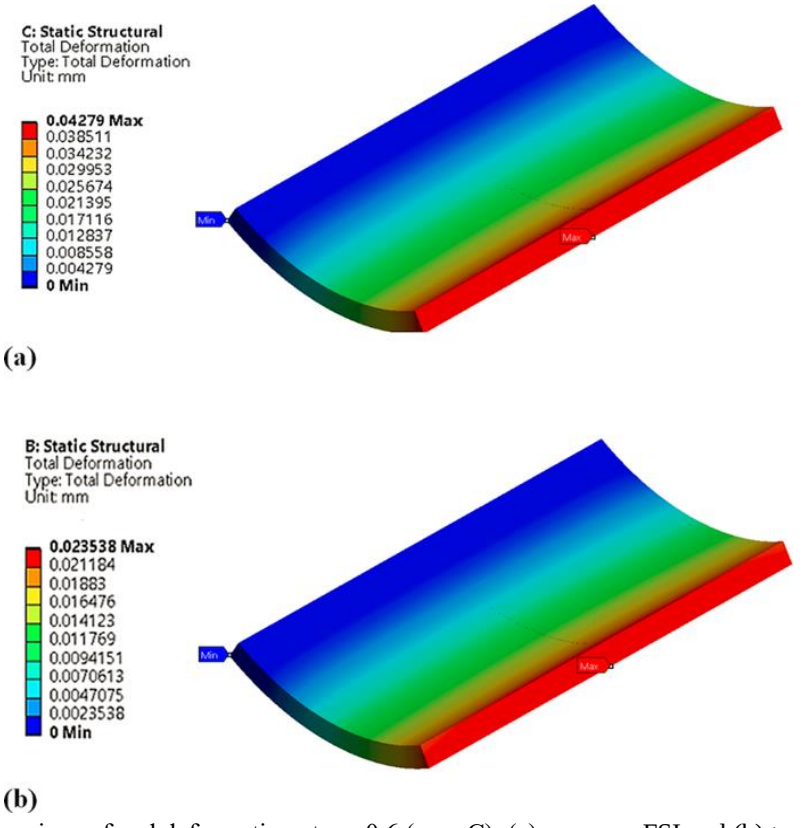

Fig. 8 Comparison of pad deformation at ε = 0.6 (case C): (a) one-way FSI and (b) two-way FSI.

observed when compared to one-way FSI. Similar trend of reduction in hydrodynamic fluid film pressures are witnessed when compared to one-way FSI for ε = 0.5 (30.64%), ε = 0.4 (51.95%), ε = 0.3 (69.44%) and ε = 0.2 (47.46%). The reason for this reduction is mainly to account for the bearing deformation that occurs due to fluid film pressure.

It can be noticed from Figs. 7(a-e) that the hydrodynamic fluid film pressure values are maximum at the region near the minimum bearing clearance, decreasing gradually on either side of the peak pressure location. Hence, for better comparison, these pressure values are extracted from the midplane of the fluid film and presented in the form of a graph for various ε as shown in Fig. S1. Fluid film pressure generated is lower near θ = 0° and θ = 60° as bearing clearance is higher, however, this pressure increases gradually and becomes maximum at the minimum clearance region. Such behavior can be observed in Fig. S1.

The pressure plots make it clear that peak hydrodynamic pressure values are lower in the two-way FSI analysis than in the one-way (Rigid bearing) study. This is mainly due to considering elastic deformation in the pad geometry. This reduction in peak hydrodynamic pressure is because of the pad deformation, and later clearance space between the journal and pad increases, enabling the lubricant to fill in the clearance region. This region acts like a lubricant reservoir and reduces the generated hydrodynamic pressure.

The fluid study showed that the fluid film pressure generated for larger ε (*i.e.*, 0.6) is higher than that for other eccentricity ratios; hence structural behavior at this eccentricity ratio is investigated. Fig. 8 compares structural deformation in the externally adjustable 60° pad bearing for both one-way and two-way FSI. In comparison, a reduction of 45% in pad deformation for two-way FSI is observed. Large deformations and higher stresses are observed along the pad's trailing edge and leading edge, respectively, because of the pad's cantilevered behavior.

Figure 9 shows the graph of max. pad deformation and max. Von-Mises stresses developed in the bearing vs. eccentricity ratio. Fig. 9(a) depicts that, for a given value of eccentricity ratio and Reynolds number (Re), deformation in the pad is on the higher side in one-way compared to two-way FSI analysis. Also, these deformations increase with the increase in eccentricity ratio. Similar observations can be made in Fig. 9(b) for Von-mises stresses. This increasing trend is mainly due to the increase in fluid film pressure, as explained earlier. Fig. 10 compares bearing load capacity results obtained from one-way and two-way FSI analysis at various eccentricity ratios for Case C (Negative radial and negative tilt adjustment). The non-dimensional load carrying capacity, $\bar{W}$ is given by Equation (6):

$$\bar{W} = W\, C / \eta\, \omega\, R^2\, L \qquad (6)$$

where, W is the load carrying capacity of bearing and ω

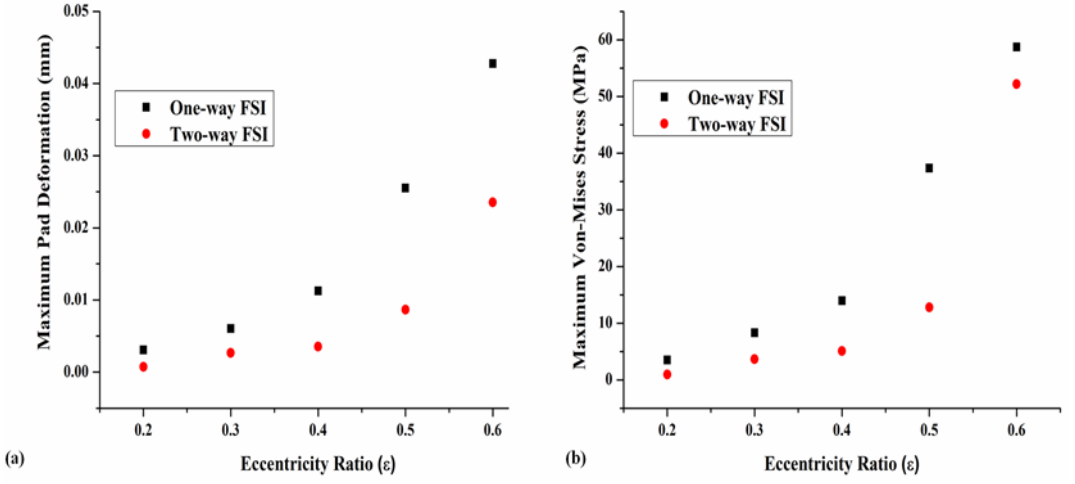

Fig. 9 Comparison of structural results for one-way FSI with two-way FSI (a) maximum pad deformation vs. eccentricity ratio and (b) maximum Von-Mises stress vs. eccentricity ratio (case C).

angular velocity of the journal.

It is quite evident from the graph that load carrying capacity obtained during two-way FSI analysis is lower compared to one-way FSI. This is caused due to the consideration of the influence of bearing deformation on lubricant in two-way FSI analysis.

4. Conclusion

FSI analysis on externally adjustable single pad fluid film bearing was presented and compared for the negative radial and negative tilt adjustment (case C). FSI technique has become a more convenient tool to evaluate the performance of fluid film bearings due to the development in computational resources. It was clear from the FSI results that for externally adjustable pad bearing with case C pad adjustment, design parameters like fluid pressure, pad deformation, and stresses were high compared to other adjustment cases. Larger fluid film pressure was mainly due to a reduction in the clearance space; hence, there would be an increase in the bearing pad deformation and stresses. It was found from the results that, in both one-way and two-way FSI analysis, the rise in design parameters was observed with the increase in eccentricity ratio. For $\varepsilon = 0.6$, the maximum fluid pressure for two-way FSI was 3.515e5 Pa, which is 60.39% greater than that for = 0.5. Similarly, larger pad deformations and stresses of 63.19% and 75.56% were observed. Similar findings were obtained from one-way FSI results. Also, one-way and two-way FSI results of EAFF bearing were compared for various eccentricity ratios for case C pad adjustments. For $\varepsilon = 0.6$, a reduction of 54.13% in the fluid film pressure and a 45% reduction in pad deformations were observed. A decrease in fluid film pressure affects the bearing performance parameter like load carrying capacity, and it is a point of concern too. A reduction of 62.85% in load carrying capacity in two-way FSI was reported for $\varepsilon = 0.6$ compared to one-way FSI. The reason is that in the two-way FSI technique, the fluid domain is allowed to change during pad deformation. These deformed pads will act like a lubricant reservoir known as pockets, reducing the fluid film pressure.

Acknowledgements

The authors thank the Department of Mechanical and Industrial Engineering, Manipal Institute of Technology, Manipal Academy of Higher Education, Manipal for providing the high computational facility to carry out this research.

Conflict of interest

The authors declare no conflict of interest.

Supporting information

Applicable.

References

[1] B. S. Shenoy, R. Pai, Stability characteristics of an externally adjustable fluid film bearing in the laminar and turbulent regimes, *Tribology International*, 2010, **43**, 1751-1759, doi: 10.1016/j.triboint.2010.04.015.

[2] I. F. Santos, F. H. Russo, Tilting-pad journal bearings with electronic radial oil injection, *Journal of Tribology*, 1998, **120**, 583-594, doi: 10.1115/1.2834591.

[3] D. C. Deckler, R. J. Veillette, M. J. Braun, F. K. Choy, Simulation and control of an active tilting-pad journal bearing, *Tribology Transactions*, 2004, **47**, 440-458, doi: 10.1080/05698190490463277.

[4] Y. Hong, D. Chen, X. Kong, J. Wang, Model of fluid-structure interaction and its application to elastohydrodynamic lubrication, *Computer Methods in Applied Mechanics and Engineering*, 2002,

191, 4231-4240, doi: 10.1016/s0045-7825(02)00376-6.
[5] B. S. Shenoy, R. S. Pai, D. S. Rao, R. Pai, Elasto-hydrodynamic lubrication analysis of full 360° journal bearing using CFD and FSI techniques, *World Journal of Modelling and Simulation*, 2010, **6**, 315-320.
[6] H. Liu, H. Xu, P. J. Ellison, Z. Jin, Application of computational fluid dynamics and fluid–structure interaction method to the lubrication study of a rotor–bearing system, *Tribology Letters*, 2010, **38**, 325-336, doi: 10.1007/s11249-010-9612-6.
[7] Y. Wang, Z. Yin, D. Jiang, G. Gao, X. Zhang, Study of the lubrication performance of water-lubricated journal bearings with CFD and FSI method, *Industrial Lubrication and Tribology*, 2016, **68**, 341-348, doi: 10.1108/ilt-04-2015-0053.
[8] Y. Chen, Y. Sun, Q. He, J. Feng, Elastohydrodynamic behavior analysis of journal bearing using fluid–structure interaction considering cavitation, *Arabian Journal for Science and Engineering*, 2019, **44**, 1305-1320, doi: 10.1007/s13369-018-3467-9.
[9] Q. Lin, Z. Wei, N. Wang, W. Chen, Analysis on the lubrication performances of journal bearing system using computational fluid dynamics and fluid-structure interaction considering thermal influence and cavitation, *Tribology International*, 2013, **64**, 8-15, doi: 10.1016/j.triboint.2013.03.001.
[10] Q. Li, G. Yu, S. Liu, S. Zheng, *Chinese Journal of Mechanical Engineering*, 2012, **25**, 926–932, doi: 10.3901/cjme.2012.05.926.
[11] K. P. Gertzos, P. G. Nikolakopoulos, C. A. Papadopoulos, CFD analysis of journal bearing hydrodynamic lubrication by Bingham lubricant, *Tribology International*, 2008, **41**, 1190-1204, doi: 10.1016/j.triboint.2008.03.002.
[12] D. A. Bompos, P. G. Nikolakopoulos, Rotordynamic analysis of a shaft using magnetorheological and nanomagnetorheological fluid journal bearings, *Tribology Transactions*, 2016, **59**, 108-118, doi: 10.1080/10402004.2015.1050137.
[13] O. O. Christidi-Loumpasefski I. Tzifas, P. G. Nikolakopoulos, C. A. Papadopoulos, Dynamic analysis of rotor–bearing systems lubricated with electrorheological fluids, *Proceedings of the Institution of Mechanical Engineers, Part K: Journal of Multi-body Dynamics*, 2017, **232**, 153–168, doi: 10.1177/1464419317725932.
[14] M. Geller, C. Schemmann, N. Kluck, Simulation of radial journal bearings using the FSI approach and a multi-phase model with integrated cavitation, *Progress in Computational Fluid Dynamics, An International Journal*, 2014, **14**, 14–23, doi: 10.1504/pcfd.2014.059196.
[15] J. K. Martin, Extended expansion of the Reynolds equation, *Proceedings of the Institution of Mechanical Engineers, Part J: Journal of Engineering Tribology*, 2002, **216**, 49-51, doi: 10.1243/1350650021543889.
[16] B. S. Shenoy, R. Pai, Steady state performance characteristics of single pad externally adjustable fluid film bearing in the laminar and turbulent regimes, *Journal of Tribology*, 2009, **131**, 1, doi: 10.1115/1.3070580.
[17] S. B. Shenoy, R. Pai, Theoretical investigations on the performance of an externally adjustable fluid-film bearing including misalignment and turbulence effects, *Tribology International*, 2009, **42**, 1088-1100, doi: 10.1016/j.triboint.2009.03.008.
[18] S. Shenoy, R. Pai, Dynamic characteristics of a single pad externally adjustable fluid film bearing, *Industrial Lubrication and Tribology*, 2011, **63**, 146-151, doi: 10.1108/00368791111126563.
[19] R. Pai, D. W. Parkins, Performance characteristics of an innovative journal bearing with adjustable bearing elements, *Journal of Tribology*, 2018, **140**, 041705, doi: 10.1115/1.4039134.
[20] H. Girish, R. Pai, Theoretical investigation of the effect of offset loads on the static characteristics of a multi-pad adjustable bearing geometry, *Australian Journal of Mechanical Engineering*, 2022, **20**, 866-874, doi: 10.1080/14484846.2020.1760435.
[21] G. Hariharan, R. Pai, Analysis on the steady state performance of a multi pad externally adjustable fluid film bearing, *Industrial Lubrication and Tribology*, 2019, **71**, 803-809, doi: 10.1108/ilt-10-2018-0371.
[22] P. Bhat, S. Shenoy B, R. Pai, Elastohydrodynamic lubrication analysis of a radially adjustable partial arc bearing using fluid structure interaction. *International Joint Tribology Conference*, 2009, **48108**, 193-195, doi: 10.1115/IJTC2007-44479.
[23] M. J. Braun, W. M. Hannon, Cavitation formation and modelling for fluid film bearings: a review, *Proceedings of the Institution of Mechanical Engineers, Part J: Journal of Engineering Tribology*, 2010, **224**, 839-863, doi: 10.1243/13506501jet772.
[24] D. Vijayaraghavan, T. G. Keith Jr, Development and evaluation of a cavitation algorithm, *Tribology Transactions*, 1989, **32**, 225-233, doi: 10.1080/10402008908981882.
[25] F. A. Martin, Discussion: "dynamically loaded journal bearings: finite element method analysis", *Journal of Tribology*, 1984, **106**, 437-438, doi: 10.1115/1.3260955.
[26] N. Zirkelback, L. San Andre´s, Finite element analysis of herringbone groove journal bearings: a parametric study, *Journal of Tribology*, 1998, **120**, 234-240, doi: 10.1115/1.2834415.
[27] W. K. Liu, S. Xiong, Y. Guo, Q. J. Wang, Y. Wang, Q. Yang, K. Vaidyanathan, Finite element method for mixed elastohydrodynamic lubrication of journal-bearing systems, *International Journal for Numerical Methods in Engineering*, 2004, **60**, 1759-1790, doi: 10.1002/nme.1022.
[28] Y. Li, R. Li, Y. Ye, X. Li, Y. Chen, Numerical analysis on the performance characteristics of a new gas journal bearing by using finite difference method, *Advances in Mechanical Engineering*, 2021, **13**, 168781402110280, doi: 10.1177/16878140211028056.
[29] J. Liu, M. Yoshihiro, Analysis of oil-lubricated herringbone grooved journal bearing with trapezoidal cross-section, using a spectral finite difference method, *Journal of Hydrodynamics*, 2010, **22**, 408-412, doi: 10.1016/S1001-6058(09)60228-6.
[30] Y. Han, S. Xiong, J. Wang, Q. Jane Wang, A new singularity treatment approach for journal-bearing mixed lubrication modeled by the finite difference method with a herringbone mesh, *Journal of Tribology*, 2016, **138**, 011704, doi: 10.1115/1.4031138.

[31] Q. Li, S. Zhang, L. Ma, W. Xu, S. Zheng, Stiffness and damping coefficients for journal bearing using the 3D transient flow calculation, *Journal of Mechanical Science and Technology*, 2017, **31**, 2083-2091, doi: 10.1007/s12206-017-0405-9.
[32] M. R. Pattnayak, R. K. Pandey, J. K. Dutt, Effects of new micro-pocketed bore surface topographies on the performance behaviours of aerodynamic journal bearing, *Surface Topography: Metrology and Properties*, 2021, **9**, 025001, doi: 10.1088/2051-672x/abefc1.
[33] G. H. Jang, D. I. Chang, Analysis of a hydrodynamic herringbone grooved journal bearing considering cavitation, *Journal of Tribology*, 2000, **122**, 103-109, doi: 10.1115/1.555333.
[34] H. Kamat, C. R. Kini, S. B. Shenoy, Numerical study of single pad externally adjustable 120° pad bearing using fluid structure interaction, *Gas Turbine India Conference*, 2021, 85536, doi: 10.1115/gtindia2021-76427.
[35] S. B. Shenoy, R. Pai, Steady state performance characteristics of a single pad externally adjustable fluid film bearing, *Journal of Advanced Mechanical Design, Systems, and Manufacturing*, 2008, **2**, 937-948, doi: 10.1299/jamdsm.2.937.
[36] D. Pan, G. Yang, H.M. Abo-Dief, J. Dong, F. Su, C. Liu, Y. Li, B. Bin Xu, V. Murugadoss, N. Naik, Vertically aligned silicon carbide nanowires/boron nitride cellulose aerogel networks enhanced thermal conductivity and electromagnetic absorbing of epoxy composites, *Nano-Micro Letters*, 2022, **14**, 118, doi: 10.1007/s40820-022-00863-z.
[37] J. C. Nicholas, Tilting pad journal bearing pivot design for high load applications, *Proceedings of the 24th Turbomachinery Symposium*, 2005, 33-48, doi: 10.21423/R1VW81.
[38] G. K. Batchelor, An introduction to fluid dynamics. Array Cambridge, UK; New York, *Cambridge University Press*, 2000.
[39] D. Y. Dhande, D. W. Pande, A two-way FSI analysis of multiphase flow in hydrodynamic journal bearing with cavitation, *Journal of the Brazilian Society of Mechanical Sciences and Engineering*, 2017, **39**, 3399-3412, doi: 10.1007/s40430-017-0750-8.
[40] C. J. Freitas, The issue of numerical uncertainty, *Applied Mathematical Modelling*, 2002, **26**, 237-248, doi: 10.1016/S0307-904X(01)00058-0.

Author Information

Mr. Harishkumar Kamat *received Mechanical Engineering from Visweswariah Technological University, Karnataka. He completed his Masters's Degree in Computer-Aided Mechanical Design and Analysis from Manipal Institute of Technology Manipal. His areas of research interest are Computational Fluid Dynamics (CFD), Fluid-Structure Interaction (FSI), and Structural Analysis. Currently, he is working as an Assistant Professor - Senior Scale in the Department of Mechanical and Industrial Engineering, Manipal Institute of Technology, Manipal.*

Dr. Chandrakant R. Kini *is a Professor in the Department of Aeronautical and Automobile Engineering, Manipal Institute of Technology, MAHE, Manipal. He has Bachelor's degree in Mechanical Engineering from Mysore University, Maters in Heat Power Engineering from National Institute of Technology Karnataka, Surathkal, and Ph. D in Turbomachinery from MAHE, Manipal, India. He has 20 years of teaching and research experience and working in MIT since 2007. In addition to teaching and research, he has been assigned additional responsibility of Assistant Director, Placement since July 2018. His area of interest are Computational Fluid Dynamics, Heat Transfer, Finite Element Method, Turbomachinery, Composite Materials, Ballistic Materials and Shock Waves. He has 40 research papers to his credit in the international journals of repute along with 15 publications in the proceedings of international and national conferences. He has reviewed journal papers for several reputed journals which includes Reviews on Advanced Materials Science, Journal of Biomechanical Engineering, Fuel, Journal of Thermal Engineering, International Review of Mechanical Engineering, Journal of Mechanical Engineering and Sciences. He is Life Member of Indian Society of Technical Education and Combustion Institute.*

Dr. Satish Shenoy B *is working as Professor in the Department of Aeronautical and Automobile Engineering at Manipal Institute of Technology, Manipal Academy of Higher Education, Manipal. He is on the mentor board of Center for Excellence in Avionics and Navigation Systems, at MIT, Manipal. He is a life member of TSI. He is an active researcher in the field Composite Structures, CFD, FEM and CAD. He has published more than 100 papers in reputed peer reviewed journals. He is on the board of reviewers of journals like Tribology International, Proceedings of the Institution of Mechanical Engineers, Part J: Journal of Engineering Tribology, Computer Methods in Biomechanics and Biomedical Engineering, Journal of the Brazilian Society of Mechanical Sciences and Engineering, Simulation Modelling Practice and Theory, Tribology Transactions, Industrial Lubrication and Tribology, Journal of Tribology, Polymer Testing, Acta Radiologica, Journal of Bionic Engineering, Journal of Marine Science and Application, Mechanics & Industry, Polymer Composites*

Publisher's Note: Engineered Science Publisher remains neutral with regard to jurisdictional claims in published maps and institutional affiliations.